WCAP-15994-NP
Revision 0

November 2002

# Structural Analysis Summary for the AP1000 Reactor Coolant Pump High Inertia Flywheel

Westinghouse

**WCAP-15994-NP**
**Revision 0**

# Structural Analysis Summary for the AP1000 Reactor Coolant Pump High Inertia Flywheel

**D. A. Wiseman**

**November 2002**

**AP1000 Document: APP-MP01-GLR-001**

Westinghouse Electric Company LLC
P.O. Box 355
Pittsburgh, PA 15230-0355

## TABLE OF CONTENTS

## LIST OF TABLES

## LIST OF FIGURES

# EXECUTIVE SUMMARY

This report summarizes the evaluation of the design of the high inertia flywheel assembly for the AP1000 reactor coolant pump. The AP1000 reactor coolant pump is a single-stage, hermetically sealed, high-inertia, centrifugal canned-motor pump. The pump motor and all rotating components are contained inside a pressure vessel.

The pump design includes flywheel assemblies in two locations to provide the inertia required for pump coastdown. Each flywheel assembly consists of a depleted uranium alloy flywheel (or insert) encased in a nickel-chromium-iron alloy (Alloy 690) enclosure. Preliminary flywheel evaluations have been completed to determine the component shrink-fit requirements, the enclosure stresses, the uranium primary stress, and the uranium critical flaw sizes. Also, missile penetration calculations were performed to evaluate the capacity of the pressure boundary structures to absorb the energy of a critical size uranium flywheel fragment in the unlikely event of a flywheel fracture.

Assembly of the flywheel structure was evaluated to ensure the torque carrying capacity of the flywheel assembly at all operating conditions.

The calculated stresses in both the uranium insert and the flywheel enclosure during both normal operating conditions (1800 rpm) and design conditions (2250 rpm) are less than the applicable stress limits.

Results of a fracture mechanics evaluation show that the critical flaw size is similar to the AP600 size.

Missile penetration calculations show that in the unlikely event of a flywheel fracture, a flywheel segment containing the maximum kinetic energy will not have sufficient energy to penetrate the pump pressure boundary structures.

# 1 INTRODUCTION

This report summarizes the evaluation of the design of the high inertia flywheel assembly for the AP1000 reactor coolant pump. The geometry analyzed is based on the overall lengths and diameters derived from the pump assembly drawing (Reference 1). The flywheel assembly design consists of a depleted uranium alloy flywheel (or insert) encased in a nickel-chromium-iron alloy (Alloy 690) enclosure. Radial shrink fits are imposed at assembly to prevent slippage due to motor torque between the shaft, the enclosure, and the uranium flywheel during pump operation. This study derives and compares stress values consistent with the non-local primary stresses reported for the AP600 evaluation (Reference 2).

The reactor coolant pump in the AP1000 design is a single-stage, hermetically sealed, high-inertia, centrifugal canned-motor pump. A canned-motor pump contains the motor and all rotating components inside a pressure vessel. The reactor coolant pump design is illustrated in Figure 3-1.

The canned-motor reactor coolant pump in the AP1000 complies with the requirement of General Design Criterion (GDC) Number 4 that components important to safety be protected against the effects of missiles. The basis for providing that the flywheel design is in compliance with the requirement of GDC 4 is outlined in subsection 5.4.1 of the AP1000 Design Control Document (DCD) (Reference 3). The licensing basis requirements include evaluation criteria for stress levels in the flywheel assembly at normal and design speeds, and for retention of the fragments by the structure of the pump following a postulated flywheel fracture. This report uses the licensing basis outlined in the AP1000 DCD (Reference 3) to establish evaluation criteria for the analysis of the flywheel.

# 2 SUMMARY OF RESULTS

The calculations and evaluations contained in this report show that the results of the AP1000 flywheel stress and missile containment studies are comparable to those of the AP600.

The applicable stress limits are derived from the American Society of Mechanical Engineers (ASME) Boiler and Pressure Vessel Code, Section III (Reference 4); the Standard Review Plan, NUREG-0800 Section 5.4.1.1 (Reference 5); and Regulatory Guide 1.14 (Reference 6). Both normal operating conditions (1800 rpm) and design conditions (125% overspeed = 2250 rpm) were evaluated. The following summarizes the results of the evaluations:

- A total advance of [ ]$^{(a,c)}$ was calculated for assembly of the flywheel structure, which ensures the torque carrying capacity of the flywheel assembly at all operating conditions.

- The calculated primary stresses in each of the uranium inserts, due to pump rotation for both normal and design conditions, are less than the allowable stress limits for the respective operating condition.

- The evaluation of the flywheel enclosure, which included assembly conditions in addition to the operating conditions, resulted in stresses in the Alloy 690 jacket that are less than allowable limits for both normal and design conditions.

- The fracture mechanics evaluation of the uranium insert indicates that for assembly plus design conditions, the critical flaw size is [ ]$^{(a,c)}$. This size is comparable to the AP600 flywheel critical flaw size of [ ]$^{(a,c)}$.

- A flywheel segment containing the maximum kinetic energy was shown to not have sufficient energy to penetrate the thermal barrier flange, which is the thinnest section adjacent to the flywheel and has the smallest capacity for penetration.

The details of the evaluations are provided in section 5.

# 3 DESCRIPTION OF COMPONENTS

The reactor coolant pump in the AP1000 design is a single-stage, hermetically sealed, high-inertia, centrifugal canned-motor pump. A canned-motor pump contains the motor and all rotating components inside a pressure vessel. The pressure vessel consists of the pump casing, thermal barrier, stator shell, and stator cap, which are designed for full reactor coolant system pressure. Two flywheel assemblies provide the required pump coastdown time. The larger of the two flywheel assemblies is located between the motor and pump impeller. This flywheel assembly is protected from direct exposure to the hot primary water by the thermal barrier. The smaller assembly is located within the canned motor below the thrust bearing. Surrounding the flywheel assemblies are the heavy walls of the casing, thermal barrier flange, motor end closure, stator shell, or flange. The reactor coolant pump concept is shown in Figure 3-1.

The flywheel assembly design consists of depleted uranium alloy inserts encased in a nickel-chromium-iron alloy (Alloy 690) enclosure. Radial shrink fits are used at assembly between the shaft, the flywheel enclosure, and the depleted uranium inserts to prevent slippage during pump operation. Flexible, full-penetration weld joints secure the end plates to the cylindrical sections of the enclosure.

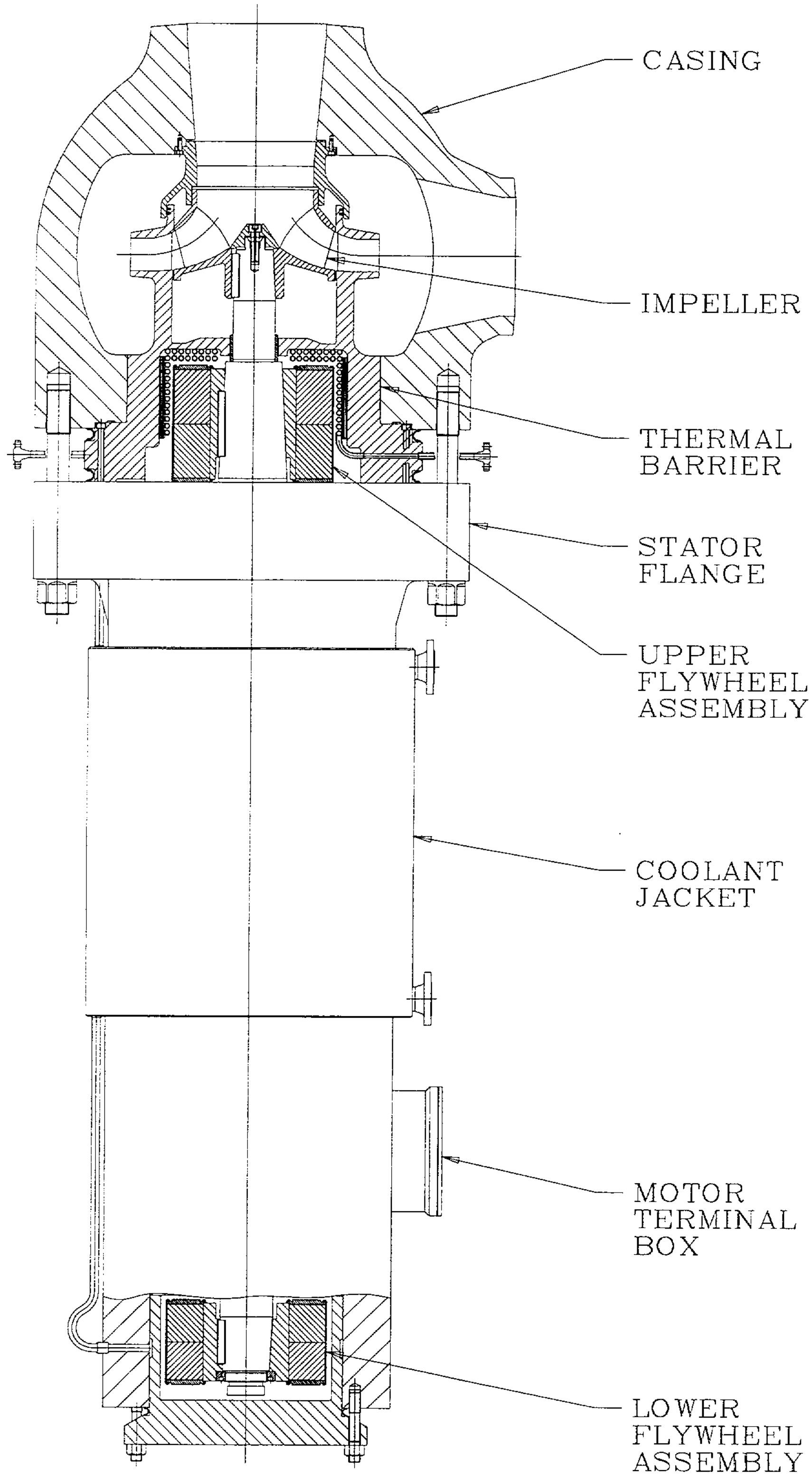


**Figure 3-1 AP1000 Canned-Motor Reactor Coolant Pump**

# 4 DESIGN REQUIREMENTS

The design requirements for the flywheel are based on the AP1000 RCP Design Specification (Reference 7) and the requirements outlined in the AP1000 DCD (Reference 3).

## 4.1 LOADING CONDITIONS

The loading conditions applicable to the flywheel are summarized below:

- Design pressure — 2500 psia
- Design temperature — 650°F for primary coolant water

  165°F assumed for bearing water
- Design speed — 2250 rpm
- Operating pressure — 2250 psia
- Operating temperature — 537°F for primary coolant water

  165°F maximum for bearing water
- Normal operating speed — 1800 rpm
- Transients — The flywheel operates in the bearing water environment that is isolated from the primary coolant by the reactor coolant pump thermal barrier. With the exception of the startup and shutdown transients, it is assumed that the primary coolant transients will have a negligible affect on the flywheel. The design specification requires that 3000 startup/shutdown cycles will be considered.
- Design mechanical loads — The AP1000 reactor coolant pump motor synchronous speed is 1800 rpm. It is required that the pump be capable of speeds up to 1.25 times the normal operating speed or 2250 rpm. There is an external applied force on the flywheel assembly enclosure due to the pump internal pressure. In addition, there are the loads associated with the shrink fits between the flywheel and the shaft, and the depleted uranium and flywheel enclosure.

## 4.2 CRITERIA

The design criteria for the flywheel assembly are given in the AP1000 RCP Design Specification (Reference 7) and are outlined in subsection 5.4.1 of the AP1000 DCD (Reference 3). The applicable stress limits are derived from the ASME Code, Section III (Reference 4), Standard Review Plan, subsection 5.4.1.1 (Reference 5), and Regulatory Guide 1.14 (Reference 6). These limits are addressed in the following subsections.

In addition to the previous criteria, the flywheel complies with the requirement of GDC 4, which requires that components important to safety be protected against the effects of missiles. It is demonstrated in section 5.2 that in the event of a postulated worst case failure, the energy of a flywheel fragment is contained by the stator shell, shell flange, thermal barrier flange, or casing shell.

### 4.2.1 American Society of Mechanical Engineers Code

The Level A stress limits of the ASME Code, Section III, Subsection NG (Reference 4) are used as evaluation criteria for the components of the flywheel assembly. Subsection NG rules and limits apply to reactor core support structures. The use of core support limits is considered appropriate for the flywheel assembly components since both the core supports and flywheel assembly operate in the reactor water environment and neither is a reactor coolant pressure boundary. An additional acceptance criterion is a limit of $S_y$ for the primary plus secondary membrane plus bending stress intensities in the main shrink-fit areas. This ensures that the flywheel will remain elastic in these areas and prevent a loss of shrink fit due to gross yielding.

### 4.2.2 Regulatory Guide 1.14

The application of the guidance of Regulatory Guide 1.14 for the analysis of the flywheel is addressed in the AP1000 DCD (Reference 3). As outlined in the DCD, the flywheel assembly is evaluated for three critical flywheel failure modes. This report demonstrates that the failure modes of ductile fracture, non-ductile fracture, and excessive preformation will not occur at the design speed (125-percent normal speed). The design speed envelopes all expected and postulated overspeed conditions, including overspeeds due to postulated pipe ruptures.

The analysis performed to evaluate the failure by ductile fracture uses the faulted stress limits in Appendix F of Section III of the ASME Code as acceptance criteria.

The enclosure is evaluated at normal operating and design speeds using the ASME Code, Section III, Subsection NG limits. The nickel-chromium-iron alloy enclosure is not evaluated for critical failure speed. The function of the enclosure is to prevent contact of reactor coolant with the uranium flywheel. No credit is taken in the evaluation of missiles from a postulated flywheel fracture for the containment of fragments by the enclosure. In addition, the enclosure contributes only a small portion of the total energy in the rotating assembly.

The analysis performed to evaluate the potential for nonductile fracture of the uranium flywheel considers the estimate of the flaw size, location, and values of fracture toughness assumed for the material. An evaluation of nonductile fracture for the uranium alloy flywheel, summarized in section 5.1, determines critical flaw size.

Failure by excessive deformation is defined as any deformation, such as an enlargement of the bore, that could cause separation directly or could cause an unbalance of the flywheel. The evaluation of excessive deformation verifies that the components of the flywheel assembly remain in contact at the design speed.

### 4.2.3 Standard Review Plan

The uranium alloy flywheel is evaluated using the stress limits given in paragraphs 4.a and 4.c of the Standard Review Plan, subsection 5.4.1.1 (Reference 5) for normal and design speed. Paragraph 4.a recommends that at normal operating speed, the combined stresses due to centrifugal forces and interference fits should not exceed 1/3 of the minimum yield strength. Paragraph 4.c recommends that at design overspeed (125 percent of normal speed), the combined stresses due to centrifugal forces and interference fit should not exceed 2/3 of the minimum specified yield strength. These limits are satisfied for the uranium alloy flywheel away from localized areas at the shrink-fit bands on the inside diameter. The shrink-fit band areas have high localized stresses, which are evaluated to the ASME Code, Section III, Subsection NG limits described in subsection 4.2.1. The Standard Review Plan limits do not apply to the nickel-chromium-iron alloy enclosure.

# 5 ANALYTICAL METHODS AND RESULTS

This section describes the components involved in the analyses, the methods of analyses for the studies, and the results.

The flywheel scoping calculations focus on determining the component shrink-fit requirements, the enclosure stresses, the uranium primary stress, and the uranium critical flaw sizes. The AP1000 flywheel segment located within the thermal barrier is similar to the AP600 design. The AP1000 has a second, smaller flywheel segment located within the canned motor below the thrust bearing. In both locations, the enclosure is isolated from the system transients and the basic design concept is the same as the AP600. Therefore, the shrink-fit requirements are similar between the AP600 and AP1000 designs. The AP1000 flywheel has the same primary stress limits as those defined for the AP600. The uranium is contained by an enclosure that also must satisfy the stress requirements of Subsection NG of the ASME Code, Section III. This study focuses on the responses of the components away from any end effects or other local stress regions.

The missile penetration calculations evaluate the capacity of the pressure boundary structures to absorb the energy of a critical size uranium flywheel fragment. The missile is not to penetrate the pressure boundary wall, so containment is preserved. This AP1000 study uses the same missile containment calculation procedure as AP600.

## 5.1 FLYWHEEL CALCULATIONS

The flywheel analyses (Reference 8) are performed by hand calculations assuming that the assembly is a stack of depleted uranium rings (called inserts) in an enclosure and shrunk onto the shaft (Figures 5-1 and 3-1). Using simplified methods, steady-state operation and 125-percent overspeed of the motor cavity flywheel are investigated. The results of these analyses are summarized as follows:

- The calculated primary stresses in each of the uranium inserts due to pump rotation are 11.69 ksi for normal conditions and 18.26 ksi for design conditions. These calculated stresses are less than the allowable stress limits for Depleted Uranium Alloy U-2Mo. Based on a material yield stress of 55 ksi, the normal condition primary stress limit is $S_y/3$=18.33 ksi and the design condition primary stress limit is $2S_y/3$ =36.67 ksi.

  The effective fit between the inner enclosure and uranium insert accommodates a radial loss of fit of approximately [ ]$^{(a,c)}$ due to rotation at 1800 rpm and the steady-state temperature of 165°F.

  The axial advance between the shaft and the inner enclosure must accommodate a radial loss of fit of approximately [ ]$^{(a,c)}$ due to rotation of 1800 rpm and the steady-state temperature of 165°F. The [ ]$^{(a,c)}$ represent an axial advance of [ ]$^{(a,c)}$. A total advance of [ ]$^{(a,c)}$ is considered in the calculations for assembly.

- The evaluations for the motor cavity flywheel are performed for steady-state conditions, which include assembly conditions, 1800 rpm of rotation, operating pressure, and a uniform temperature of 165°F, as well as for assembly conditions plus 125-percent overspeed at 70°F. In the

[ ][(a,c)] outer enclosure (jacket) at steady-state conditions, the hoop stress is 18.71 ksi, and for the 125-percent overspeed condition, the jacket hoop stress is 21.34 ksi. Note that for the Alloy 690 jacket, these calculated hoop stresses are less than the respective yield stresses of 32.5 ksi at 165°F and 35 ksi at 70°F. The primary plus secondary stress intensity for shrink-fit components is limited to $S_y$ to preclude loss of shrink due to gross yielding.

- A preliminary fracture mechanics evaluation of the AP1000 uranium insert for sudden rupture indicates that for steady-state pump operation, the critical flaw size is [ ][(a,c)]. For assembly plus 125-percent overspeed, the critical flaw size is reduced to [ ][(a,c)]. These flaw sizes compare favorably with the AP600 design critical flaw size of [ ][(a,c)].

### 5.1.1 Analytical Model

The calculations for the AP1000 motor cavity flywheel assembly are performed via hand calculations considering a series of concentric rings shrunk fit together to make the assembly. These rings and pertinent geometrical properties are illustrated in Figure 5-1. For the present analyses, the material for the rotor shaft is 403 stainless steel, the inner enclosure and jacket are assumed to be Alloy 690, and the uranium insert is Depleted Uranium Alloy U-2Mo. The concentric rings are evaluated for assembly conditions, shaft rotation at 1800 rpm, pressure loading, and a steady-state temperature of 165°F.

The mechanical properties for the flywheel are presented in Table 5-1. The properties for 403 stainless steel and the Alloy 690 components are taken from the ASME Code. The depleted uranium properties are from the AP1000 RCP Design Specification (Reference 7).

**Table 5-1 Mechanical Properties**

| Component | Modulus (psi) | Expansion Coefficient (/°F) | Density lb/in³ |
|---|---|---|---|
| Shaft | $E_S = 29.2x10^6$ | $\alpha_S = 6.13x10^{-6}$ | $\rho_S = 0.280$ |
| Inner enclosure | $E_I = 30.3x10^6$ | $\alpha_I = 7.83x10^{-6}$ | $\rho_S = 0.304$ |
| Uranium | $E_U = 21.5x10^6$ | $\alpha_U = 9.11x10^{-6}$ | $\rho_S = 0.688$ |
| Jacket | $E_J = 30.3x10^6$ | $\alpha_J = 7.83x10^{-6}$ | $\rho_S = 0.304$ |

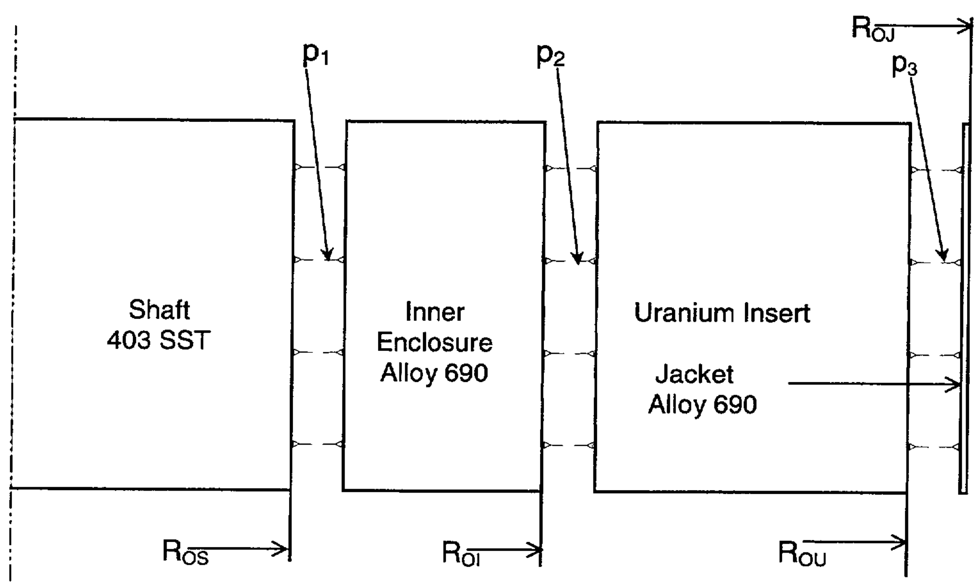


$p_1$ = the interface pressure between the shaft and the inner enclosure
$p_2$ = the interface pressure between the inner enclosure and the uranium
$p_3$ = the interface pressure between the uranium and the jacket
$R_{OI}$ = the inner enclosure outer radius and the uranium inner radius
$R_{OJ}$ = the jacket outer radius
$R_{OS}$ = the shaft outer radius and the inner enclosure inner radius
$R_{OU}$ = a uranium insert outer radius and the jacket inner radius

[ ] (a,c)

**Figure 5-1 Flywheel Assembly Dimensions**

### 5.1.2 Concentric Ring Model Geometry and Material Properties Shrink-Fit Effects

The flywheel assembly will be manufactured by initially shrink fitting the uranium inserts onto the Alloy 690 inner enclosure and then shrink fitting the jacket onto the insert/enclosure assembly, and welding the jacket to the upper and lower cover plates. Note that for the inner enclosure to insert shrink fit, the inner radius of the enclosure displaces approximately [ ]$^{(a,c)}$ due to the shrink of the uranium inserts. The outer radius of the insert displaces approximately [ ]$^{(a,c)}$ for each mil of radial shrink between these components. Prior to shrinking the jacket onto the inserts, the displacement of the inserts must be taken into account to insure that the jacket will not be overstressed during the shrink operation. [

]$^{(a,c)}$ Additionally the interface pressure between the inserts and the jacket increases due to advancing the flywheel onto the shaft.

In order to prevent slippage between components that could change the balance of the flywheel, sufficient shrink fit must be maintained to carry the maximum rotational acceleration of the flywheel. Loads were conservatively calculated using the torque of the motor. The calculations show that a total axial advance of [ ]$^{(a,c)}$ in the assembly of the flywheel results in the maintenance of some interference fit during all load conditions, including design speed. These results demonstrate conformance with the Regulatory Guide 1.14 recommendation relative to the excessive deformation failure mode.

### 5.1.3 Uranium Insert Rotational Primary Stresses

Per the AP1000 RCP Design Specification (Reference 7), the design speed of the flywheel is defined as 125% of the normal speed of the motor. At normal speed the calculated maximum primary stresses in the uranium flywheel shall be limited to less than $1/3S_y$. At the design speed the calculated maximum primary stress in the uranium flywheel shall be limited to less than $2/3S_y$. The calculations for these primary stresses due to rotation consider only the uranium portion of the flywheel assembly and do not include any of the stresses due to component shrink fit or axial advance of the impeller onto the shaft.

The maximum primary stress in the uranium inserts is the hoop stress at the inner radius of the insert. The calculations for the hoop stress are given as follows:

- Uranium insert inner radius hoop stress

$$\sigma_{\theta\theta}(R_{OI})_U = \frac{\rho_U \omega^2}{4g}\left[(3+\nu)R_{OU}^2 + (1-\nu)R_{OI}^2\right]$$

- Uranium insert normal operation inner radius hoop stress

$$\sigma_{\theta\theta}(R_{OI})_U = \frac{0.688\frac{lb}{in^3}\left(188.5\frac{rad}{sec}\right)^2}{4\times 386.4\frac{in}{sec^2}}\left[(3+\nu)(14.50in)^2+(1-\nu)(8.00in)^2\right]=11685\,psi$$

- Uranium insert design condition inner radius hoop stress

$$\sigma_{\theta\theta}(R_{OI})_U = \frac{0.688\frac{lb}{in^3}\left(1.25\times 188.5\frac{rad}{sec}\right)^2}{4\times 386.4\frac{in}{sec^2}}\left[(3+\nu)(14.50in)^2+(1-\nu)(8.00in)^2\right]=18255\,psi$$

The uranium insert is Depleted Uranium Alloy U-2Mo, and the yield stress for this material is 55,000 psi. Per the design specification, the $1/3S_y$ is 18,330 psi and $2/3S_y$ is 36,670 psi. For normal operation at a rotational speed of 1800 rpm, the maximum primary hoop stress is 11,685 psi, which is less than 18,330 psi. Additionally, for a design rotational speed of 2250 rpm, the maximum primary hoop stress is 18,255 psi, which is less than 36,670 psi. Since the rotational stresses for the uranium flywheel are less than the prescribed allowable stresses, the requirements of the design specification are satisfied.

### 5.1.4 Concentric Ring Elastic Hoop Stresses

In Table 5-2, the hoop stresses at the inner and outer diameter of each of the concentric rings in the model are presented for assembly conditions, 1800 rpm of rotation, operating pressure, and a uniform temperature of 165°F, as well as for assembly conditions and 125-percent overspeed at 70°F. From Table 5-2, it is noted that the hoop stresses of 18.71 ksi and 21.34 ksi in the jacket are less than the yield stresses for Alloy 690, which are 32.5 ksi at 165°F and 35 ksi at 70°F.

**Table 5-2 AP1000 Motor Cavity Flywheel Hoop Stresses**

| | Shaft | | Inner Enclosure | | Uranium | | Jacket | |
|---|---|---|---|---|---|---|---|---|
| | Inner Radius $S_{ttSI}$ (psi) | Outer Radius $S_{ttSO}$ (psi) | Inner Radius $S_{ttII}$ (psi) | Outer Radius $S_{ttIO}$ (psi) | Inner Radius $S_{ttUI}$ (psi) | Outer Radius $S_{ttUO}$ (psi) | Inner Radius $S_{ttJI}$ (psi) | Outer Radius $S_{ttJO}$ (psi) |
| **Steady-State Operation** | | | | | | | | |
| Assembly(1) | -13483 | -13483 | -5634 | -7826 | 20338 | 9338 | 16996 | 16705 |
| 2335 psi | -2500 | -2500 | -2566 | -2547 | -2027 | -2198 | -2809 | -2801 |
| 1800 rpm | 5014 | 4842 | 4971 | 4700 | 3713 | 1978 | 2781 | 2704 |
| 165°F | 2857 | 2857 | -1961 | -616 | -2920 | -1379 | 1745 | 1715 |
| Total | -8111 | -8284 | -5191 | -6289 | 19105 | 7740 | 18713 | 18324 |
| **125-Percent Overspeed at 70°F** | | | | | | | | |
| Assembly(1) | -13483 | -13483 | -5634 | -7826 | 20338 | 9338 | 16996 | 16705 |
| 0 psi | 0 | 0 | 0 | 0 | 0 | 0 | 0 | 0 |
| 2250 rpm | 7835 | 7565 | 7767 | 7344 | 5802 | 3091 | 4346 | 4225 |
| 70°F | 0 | 0 | 0 | 0 | 0 | 0 | 0 | 0 |
| Total | -5648 | -5918 | 2133 | -481 | 26140 | 12429 | 21342 | 20931 |

1. Axial Advance, $\Delta$ = [ ]$^{(a,c)}$, Insert/Inner Enclosure Radial Shrink $\sigma_{SUI}$ = [ ]$^{(a,c)}$, Jacket/Insert Radial Shrink $\sigma_{SUJ}$ = [ ]$^{(a,c)}$

### 5.1.5 Fracture Mechanics of Uranium Insert

An estimate of the critical flaw sizes in the uranium insert is made using the approach from section 6.4 of WCAP-13734 (Reference 2). For the present calculations, the sudden rupture of the uranium insert is governed by the critical Mode I (tensile) fracture toughness of the material, namely $K_{IC}$ = 50 ksi. in$^{1/2}$. The hoop stress distribution across the uranium insert and the critical crack sizes are presented in Table 5-3 for steady-state operation and assembly plus 125-percent overspeed. These crack sizes are estimated using Version 3.0 of NASCRAC (NASA Crack Analysis Code by Failure Analysis Associates, Inc., of Palo Alto, California). For these estimates, Case 205 represents a full-length axial crack on the inner diameter of a hollow cylinder. Additionally, Case 704 is a semi-elliptical axial surface flaw in a cylinder, and for this case, flaws with aspect ratios of 1:1 and 3:1 are considered. From Table 5-3, the minimum flaw size is [ ]$^{(a,c)}$ for assembly + 125-percent overspeed. These results can be used to support fracture toughness and inspection requirements for the uranium alloy material.

**Table 5-3 AP1000 Uranium Insert Hoop Stress Distribution and Critical Crack Size Summary**

| Insert Radial Locations (inch) | Steady-State Operation | Assembly + 125-Percent Overspeed |
|---|---|---|
| [ ](a,c) | 19.10 ksi | 26.14 ksi |
| | 14.60 ksi | 20.90 ksi |
| | 11.65 ksi | 17.37 ksi |
| | 9.48 ksi | 14.68 ksi |
| | 7.74 ksi | 12.43 ksi |
| NASCRAC Case crack size | 205 [ ](a,c) | 205 [ ](a,c) |
| NASCRAC Case crack size | 704 (1:1) [ ](a,c) | 704 (1:1) [ ](a,c) |
| NASCRAC Case crack size | 704 (3:1) [ ](a,c) | 704 (3:1) [ ](a,c) |

## 5.2 MISSILE PENETRATION

This analysis (References 8 and 9) follows the same procedure used for turbine disk fractures in Reference 10. Although no significant flaws are expected in the uranium and the material is not really brittle ($K_{IC}$ = 50 ksi. $in^{1/2}$ per Reference 11), this analysis assumed a fracture has occurred and shows that the energy of the fragments is insufficient to penetrate the pressure boundary. No other effects of a flywheel failure were considered in this evaluation.

### 5.2.1 Assumptions

The method of analysis of Reference 10, which was developed from scale tests of turbine disks, is considered applicable herein with the following conservative assumptions used.

- The outer Alloy 690 enclosure of the flywheel was neglected. In reality, this enclosure would need to be breached in the unlikely event of a uranium flywheel fracture before the pressure boundary being impacted by the fragment. This analysis completely ignored the Alloy 690 components.
- The Alloy 690 end plates/welds and the surrounding water were also neglected from the energy absorption calculations.
- The minimum ASME material strength properties at temperature were used for the pressure boundary (containment closure). The pressure boundary material is taken to be CF8 or F304 SS @ 550°F.
- Only one of the disk segments was considered to fail.

- No secondary effect of the shrink fit of the uranium flywheel to the shaft was considered.
- The shell containment in line with the flywheel segment was the only containment material considered.
- The design speed of 125 percent times the operating speed of 1800 rpm was used.

This is the same approach as used in the AP600 analysis (Reference 2).

### 5.2.2 Energy Analysis

The containment of disk fragments by a cylindrical shell is a two-stage process, per Reference 10. The first stage involves inelastic impact and transfer of momentum to the containment cylinder. If the energy dissipated in plastic compression and shear strain is sufficient to accommodate the loss of kinetic energy of the flywheel, there is no shear perforation of the shell. The process then enters Stage 2, which involves dissipation of energy in plastic tensile strain in the shell. For containment, the energy dissipated in plastic tensile strain must accommodate the residual kinetic energy of the flywheel. Note the procedure has experimental verification of the analytical techniques (Reference 10). The kinetic energy of a fragment is:

$$\frac{1}{2} M V^2 \text{, where M = mass of fragment and V = fragment velocity after rupture}$$

Fragment rotational considerations can be neglected per Reference 10. The flywheel could burst into halves, thirds, quarter fragments, or even pieces. Reference 10 typically used quarter fragments in testing, but for penetration considerations, it was shown that the kinetic energy is a maximum value for a 134° sector. As the fragment mass increases, the radius (r) to the fragment center of gravity decreases. Since a 134° mass would represent the maximum energy case for penetration, this is taken as the limiting case. A 134° flywheel sector was also assumed in the flywheel containment calculations for the AP600 reactor coolant pump (Reference 2).

Four cases of the containment shell model are considered. Case A is through the thermal barrier flange material, Case B is through the pump casing, Case C is through the thickest section of the combined thermal barrier and casing flanges, and Case D is through the lower stator shell. The analysis model gives the containment thickness of the four cases in Table 5-4.

**Table 5-4 Pump Containment Thicknesses Analyzed in Missile Analysis**

| Case | Inner Radius (inch) | Outer Radius (inch) | Thickness (inch) | |
|---|---|---|---|---|
| A | [ | | ] | (a,c) |
| B | | | | |
| C | | | | |
| D | [ | | ] | |

### 5.2.3 Missile Containment Analysis Results

The pressure boundary sections contain the uranium flywheel fragment with the greatest kinetic energy. The verified semi-empirical method of Reference 10 shows that any improbable flywheel fracture would not penetrate the thermal barrier flange or the casing assembly that surround the larger flywheel assembly located within the thermal barrier region. The location of the smaller flywheel segment in the canned motor is such that the stator wall/flange, which acts as the containment for a flywheel failure in this area, is at least as thick as the minimum wall analyzed for the flywheel assembly located within the thermal barrier region (Case A). Therefore, the smaller flywheel segment (Case D) will also not penetrate the surrounding stator wall in the unlikely event of a flywheel fracture.

The following Table 5-5 compares the fragment energy to the energy available for the Stage 1 (shear) penetration and for the Stage 2 (tensile) penetration. The ratio of the two gives the third column of results that is presented as a percentage of capacity.

### 5.2.4 Conclusion

The analysis shows that even in the unlikely event of the flywheel failure, any loose parts (missiles) will be contained within the primary pressure boundary.

**Table 5-5 Pressure Boundary Capacity for Missile Containment**

| Case | Fragment Energy (ft-lb) | Energy Required for Penetration (Boundary Capacity) (ft-lb) | Percentage of Available Capacity |
|---|---|---|---|
| Case A - Stage 1 | 290,947 | 5,788,145 | 5.0 |
| - Stage 2 | 293,257 | 2,487,511 | 11.8 |
| - Total | 584,204 | 8,275,656 | 7.1 |
| Case B - Stage 1 | 368,203 | 7,951,997 | 4.6 |
| - Stage 2 | 216,002 | 4,275,407 | 5.0 |
| - Total | 584,205 | 12,227,404 | 4.8 |
| Case C - Stage 1 | 452,620 | 44,206,334 | 1.0 |
| - Stage 2 | 131,584 | 8,626,976 | 1.5 |
| - Total | 584,204 | 52,833,310 | 1.1 |
| Case D - Stage 1 | 170,869 | 5,936,300 | 2.9 |
| - Stage 2 | 179,654 | 1,582,198 | 11.4 |
| - Total | 350,523 | 7,518,498 | 4.7 |

# 6 REFERENCES

1. APP-MP01-V1-001, "AP1000 Rector Coolant Pump Outline."

2. WCAP-13734, "Structural Analysis Summary for the AP600 Reactor Coolant Pump High Inertia Flywheel," May 1993.

3. APP-GW-GL-700, "AP1000 Design Control Document," subsection 5.4.1.

4. ASME Boiler and Pressure Vessel Code, Section III, Subsection NG and Appendices, 1998 Edition, American Society of Mechanical Engineers, New York, N.Y.

5. NUREG-0800, "Standard Review Plan," Revision 1, Section 5.4.1.1, U.S. Nuclear Regulatory Commission, Office of Nuclear Regulation, Washington, D.C., July 1981.

6. Regulatory Guide 1.14, Revision 1, "Reactor Coolant pump Flywheel Integrity," U.S. Nuclear Regulatory Commission, Office of Standard Development, Washington, D.C., August 1975.

7. APP-MP01-M2-001, "AP1000 RCP Design Specification."

8. Dietrich, D. E., "AP1000 RCP Concept Design Flywheel Scoping, Missile Containment, and Rotor Critical Speed Calculations," Westinghouse Government Services Company LLC, Electro-Mechanical Division, Analytical Technologies Letter AT/S-02-17, Revision 1, May 21, 2002.

9. Brose, W. R. and Dietrich, D. E., "Updated Analysis of Missile Containment for AP1000 RCP Concept Design Flywheel," Curtiss-Wright Electro-Mechanical Corporation, Analytical Technologies Letter AT/S-02-40, November 21, 2002.

10. Hagg, A. C., and Sankey, G. O., "The Containment of Disk Burst Fragments by Cylindrical Shells," ASME Paper 73-WA-Pwr-2, 11/73; also in ASME Journal of Engineering for Power, 4/74, pg. 114-123.

11. Deel, O. L., and R. J. Burian, "The Mechanical Properties of Depleted Uranium –2% Molybdenum Alloy," Battelle Lab Report BMI-2032(UC-71), July 16, 1979.